The 2015 World Congress on
Advances in Civil, Environmental, and Materials Research (ACEM15)
Incheon, Korea, August 25-29, 2015

FE Meshing Scheme for Accurate Placement/Area of PZT Actuators for Flutter Damping Using LQR Method

Sallam A. Kouritem[1)], Mohamed M Y. B. Elshabasy[2)] and Hassan A. El-Gamal[3)]

[1), 2), 3)] *Department of Mechanical Engineering, Alexandria University,*
Teaching assistant at faculty of engineering, Alexandria, Egypt
[1)] sallam_keritemya@yahoo.com

ABSTRACT

In this paper, to choose the optimum aspect ratio in the Finite element formulation of aircraft panel flutter simulation and damping, a standard square panel of embedded piezoelectric (PZT) actuator is investigated. The model formulation is based on the first-order shear deformation theory for laminated panel and the Von-Karman large deflection strain displacement relations. The aerodynamic loading is calculated using the quasi-steady first piston theory. Besides, the linear piezoelectricity constitutive relations are used. Nonlinear equations of motion are obtained using the four-node Bogner Fox-Schmit (BFS) rectangular plate element and the electrical degree of freedom is presented to model piezoelectric actuator. The modal transformation is used to decrease the time consumed in solving system of nonlinear equations. A Linear Quadratic Regulator (LQR) full state feedback is designed to obtain the suitable gain factors to achieve the desired damping. The optimal size and location of piezoelectric actuators to improve the flutter suppression are determined using the norm feedback control gain (NFCG) method. It is very important to select suitable finite element meshing size for high control authority of smaller PZT actuator area. Thus, once the optimum aspect ratio is determined, a lighter PZT embedded panel, smaller PZT area and less power to be consumed take place.

Keywords: Flutter; Damping; Piezoelectric; Finite Element; Aspect Ratio; Optimum, Norm Feedback Control Gain, Linear Quadratic Regulator.

INTRODUCTION

Supersonic Panel flutter is a self-excited oscillation of a plate or shell when exposed to airflow along its surface. In 1965, (Johns 1965) presented a survey of panel flutter and related research in NATO countries. (Mei, Abdel-Motagaly et al. 1999) provided a review of nonlinear panel flutter at supersonic and hypersonic speeds. (Chowdary, Parthan et al. 1994) used the finite element method using a quadratic isoparametric element to study the free vibration and flutter characteristics of laminated composite panels. (Raja, Pashilkar et al. 2006) proved that flutter speed can be delayed using piezoelectric actuator. (Zhou, Xue et al. 1994) classified the panel flutter behavior into different five types, which includes flat,

buckled, limit-cycle, periodic and chaotic motions for different values of nondimensional aerodynamic pressure and it's critical value (Forster and Y. Yang 1998) used the piezoelectric actuator to control flutter of aluminum wing boxes. (lock 1961) Studied the flutter of two dimensional flat panels and used the ideal flutter theory to predict the boundaries of these panels. (Pidaparti 1993) used a 48 degrees of freedom doubly curved quadrilateral thin shell finite element in the investigation of the supersonic flutter of cantilevered curved composite panels. (Yucheng Shi 1999) presented a formulation based on the FEM in modal coordinates for solving thermal post buckling drawbacks. The deflection shape change was observed and participation of each mode was described.

(Moon, Yun et al. 2002; Moon 2006) used the genetic algorithm (G.A) to determine the optimal shape and location of the piezoelectric sensors and actuators for maximum control authority. (S.X. Xu 2004) found that the location of piezoelectric sensors and actuators had significant influence on the integrated system and control performance. (Bin Zheng 2012) showed that the vibration control can be enhanced by increasing the number of the (PZT) bonded actuators. (M. Lotfy 2009) found that the control effect of piezoelectric material patches increases as long as they are placed away from the panel boundary. (Lee, Yuen et al. 2002) showed that the optimal piezoelectric actuator size depends on the excitation level. For higher excitation level, optimal actuator size is larger. (Abdel-Motagaly 2001; Otiefy and Negm 2011) and Abdel-Motagaly (Abdel-Motagaly 2001) determined the optimum locations of actuators and sensors using the norm of feedback control gains (NFCG) and norm of Kalman filter estimator gains (NKFEG).

In the first half of 2013, an overwhelming number of panel flutter related researches were conducted. For example, (Li and Narita 2013) demonstrated that the increasing of the aerodynamic cause the buckling occurs before the flutter. (Vedeneev) performed the calculations of panel flutter boundaries at low supersonic speeds considering the panel damping. (Li and Song 2013) analyzed the aero-thermoelastic properties of laminated panels and investigated the flutter and thermal buckling control of the structural system. (Sallam ahmed kouritem 2013) proposed an ad-hock iterative search method to determine the optimal size and location of piezoelectric actuators to damp the flutter suppression in a short time.

In the current investigation, we shed the light on the effect of meshing aspect ratio of the finite element formulation in the panel flutter simulation and damping using PZT on the optimum placement and area of the PZT actuator. Accordingly, the power consumed in flutter damping will be extensively reduced. The paper is composed of seven sections. The finite element formulation is explained in the first section. The second section contains the modal formulation. The control design to determine the control gain factor is presented in the third section. The fourth section is about the modal participation. The fifth section is the numerical simulations of nonlinear panel flutter for a square isotropic panel at various meshing sizes. In the sixth section placement methodology of piezoelectric actuator is discussed. The investigation is concluded in the seventh section.

FINITE ELEMENT FORMULATION

The Finite element formulation is used to simulate the dynamic response of the aluminum panel integrated with embedded PZT actuators at an arbitrary location.

Modified Rectangular Plate Element

In the current study, the Bogner-Fox-Schmit (BFS) C^1 (Zhou, Mei et al. 1996; qinqin 2005) conforming rectangular elements is used in the modeling. Each BFC element consists of 16 bending degree of freedom (DOF) and eight in-plane degree of freedom (DOF). The electrical degree of freedom is assumed to be constant throughout the plan area of each piezoelectric layer and to vary linearly through the thickness. The electrical degrees of freedom can be expressed as:

$$\{w_\varphi\} = \{V_1, V_2, \dots, \quad V_{np}\} \tag{1}$$

Where; the V_i is the electric potentials applied to or detected from the piezoelectric layers of the element, and np denotes the total number of piezoelectric layers composing the PZT actuator. In the current investigation, np = 2 (bonded up and down back –to-back) to augment the bending effect and eliminate the in-plane force through applying a voltage of opposite polarity to one of the PZT poling voltage and another voltage of the same polarity of the other PZT layer bonded to the other side of the hosting panel.

Constitutive Equations

In the derivation of equations of motion, the panel is assumed thin such that the rotary inertia and transverse shear deformation effects are neglected. The Von-Karman nonlinear strain-displacement relations are expressed as:

$$\begin{Bmatrix} \varepsilon_x \\ \varepsilon_y \\ \gamma_{xy} \end{Bmatrix} = \{\varepsilon_m^0\} + \{\varepsilon_\theta^0\} + z\{k\} = \begin{bmatrix} u_{,x} \\ v_{,y} \\ u_{,y} + v_{,x} \end{bmatrix} + \frac{1}{2}\begin{Bmatrix} w_{,x}^2 \\ w_{,y}^2 \\ 2w_{,x}w_{,y} \end{Bmatrix} + z\begin{Bmatrix} -w_{,xx} \\ -w_{,yy} \\ -2w_{,xy} \end{Bmatrix} \tag{2}$$

Where u and v are the in-plane displacements. The membrane strains $\{\varepsilon_{\mathrm{m}}^0\}$ and $\{\varepsilon_{\theta}^0\}$ are due to in-plane displacements and large deflections, respectively.

For an aircraft panel consisting of hosting panel and piezoelectric layers, the stress-strain relationships for a general k_{th} layer, can written as

$$\begin{Bmatrix} \sigma_x \\ \sigma_y \\ \tau_{xy} \end{Bmatrix}_k = \begin{bmatrix} [\bar{Q}_{11}] & [\bar{Q}_{12}] & [\bar{Q}_{16}] \\ [\bar{Q}_{12}] & [\bar{Q}_{22}] & [\bar{Q}_{26}] \\ [\bar{Q}_{16}] & [\bar{Q}_{26}] & [\bar{Q}_{66}] \end{bmatrix}_k \left\{ \begin{Bmatrix} \varepsilon_x \\ \varepsilon_y \\ \gamma_{xy} \end{Bmatrix} - E_{3k} \begin{Bmatrix} d_x \\ d_y \\ d_{xy} \end{Bmatrix}_k \right\} \tag{3}$$

For piezoelectric layers, the corresponding electric displacements are only detected along the poling axis. The electrical displacement for the k_{th}layer can expressed as [22]

$$D_{3k} = \begin{bmatrix} d_x d_y d_{xy} \end{bmatrix}_k \begin{bmatrix} [\bar{Q}_{11}] & [\bar{Q}_{12}] & [\bar{Q}_{16}] \\ [\bar{Q}_{12}] & [\bar{Q}_{22}] & [\bar{Q}_{26}] \\ [\bar{Q}_{16}] & [\bar{Q}_{26}] & [\bar{Q}_{66}] \end{bmatrix}_k \left(\begin{Bmatrix} \varepsilon_x \\ \varepsilon_y \\ \gamma_{xy} \end{Bmatrix} - E_{3k} \begin{Bmatrix} d_x \\ d_y \\ d_{xy} \end{Bmatrix}_k \right) + \varepsilon_{33k}^{\sigma} E_{ik} \qquad (4)$$

Where $[\bar{Q}]_k$and $\{d\}_k$ are the lamina stiffness and stress/charge constants, respectively. The resultant forces and moments acting on a laminate (as shown in figure 1) are obtained by integration of the stresses resultants, per unit length in each layer or laminate through the lamina thickness, h.

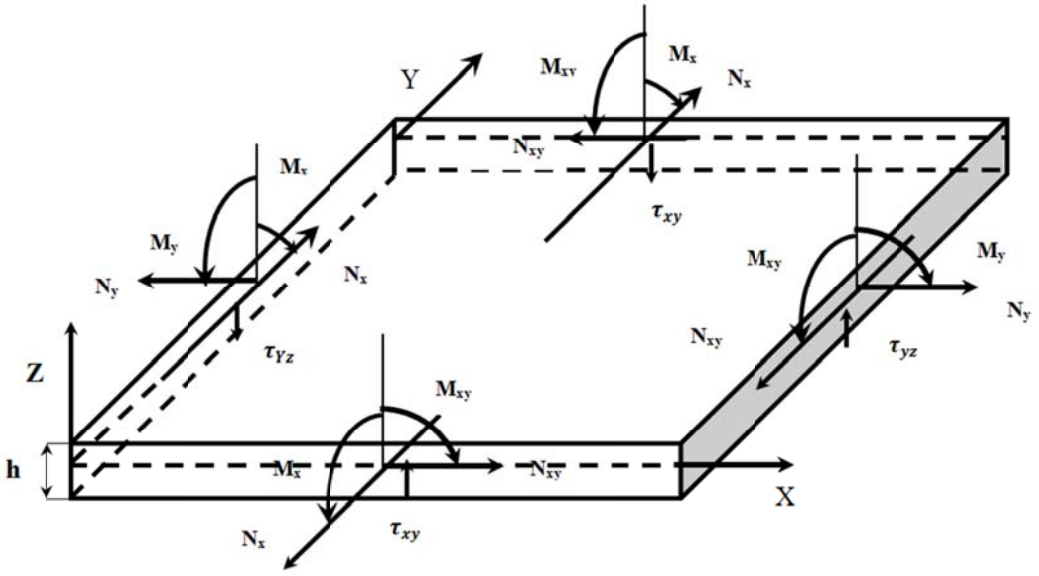

Figure 1 The Resultant Forces and Moments Acting on a Laminate

$$(\{N\}, \{M\}) = \int_{-h/2}^{h/2} \{\sigma\}_k \, (1, z) \, dz \qquad (5)$$

Which, lead to the constitutive relations for a laminated panel:

$$\begin{Bmatrix} N \\ M \end{Bmatrix} = \begin{bmatrix} [A] & [B] \\ [B] & [D] \end{bmatrix} \begin{Bmatrix} \varepsilon^0 \\ k \end{Bmatrix} - \begin{Bmatrix} N_{\emptyset} \\ M_{\emptyset} \end{Bmatrix} \qquad (6)$$

The laminate stiffness matrices are given by:

$$[A] = \sum_{k=1}^{n} [\bar{Q}]_k \, (z_{k+1} - z_k)$$
$$[B] = \sum_{k=1}^{n} \frac{1}{2} [\bar{Q}]_k \, (z_{k+1}^2 - z_k^2) \qquad (7)$$
$$[D] = \sum_{k=1}^{n} \frac{1}{3} [\bar{Q}]_k \, (z_{k+1}^3 - z_k^3)$$

The piezoelectric in-plane force $\{N_\emptyset\}$, is set zero. This is achieved by having a single piezoelectric layer that is used as actuator and sensor simultaneously (Abdel-Motagaly, Guo et al. 2005) .

First-Order Piston Aerodynamic Theory

For panel flutter at high supersonic flow first-order piston theory (Zhou, Mei et al. 1996; Abdel-Motagaly, Guo et al. 2005; qinqin 2005) is commonly used.
The aerodynamic pressure can be written as:

$$P_a = -\frac{2q}{\beta}\left[\frac{\partial w}{\partial x} + \frac{M_\infty^2 - 2}{M_\infty^2 - 1}\frac{1}{V}\frac{\partial w}{\partial t}\right] = -\left[\lambda \frac{D_{110}}{L^3}\frac{\partial w}{\partial x} + \frac{g_a}{w_0}\frac{D_{110}}{L^4}\frac{\partial w}{\partial t}\right] \qquad (8)$$

Where; P_a is the aerodynamic pressure, V is the airflow velocity, M_∞ is the mach number, $q = \frac{1}{2}\rho_a V^2$ is the dynamic pressure, ρ_a is the air mass density, $\beta = \sqrt{M_\infty^2 - 1}$, w is the panel lateral displacement. For composite plates, D_{110} is the first element in the laminate bending stiffness matrix D calculated when all the fibers of the composite plate are aligned in the x-direction; L is the panel length.

$$\lambda = \frac{2qL^3}{\beta D_{110}}, \; \mu = \frac{\rho_a}{\rho h}, \; C_a = \left(\frac{M_\infty^2 - 2}{M_\infty^2 - 1}\right)^2 \frac{\mu}{\beta}, \; g_a = \frac{\rho_a V \, (M_\infty^2 - 2)}{\beta^3 \, \rho h w_o} = \sqrt{\lambda C_a}, \; w_0 = \sqrt{\frac{D_{110}}{\rho h L^4}} \qquad (9)$$

Where; λ is the non-dimensional dynamic pressure; μ is the mass ratio; g_a is non-dimensional aerodynamic damping, and C_a is its coefficient; and w_0 is a reference frequency.

Equations of Motion

Using the Hamilton's principle (Li 2012) and (qinqin 2005) the finite element equations for the laminated composite plate with fully coupled electrical-structural properties can be derived from

$$\int_{t_1}^{t_2} \delta(T - U + W_e) = 0 \tag{10}$$

Where T and U are respectively the kinetic and strain energy of the system, $W_e$is express the electrical energy and t_1 and$t_2$are the integration limits. After substitution for T, U and W_e into Eq. (10).

$$\int_V [\rho(\delta\dot{w}^T\dot{w} + \delta u^{\cdot T}\dot{u} + \delta\dot{v}^T\dot{v}) - \{\delta\epsilon\}^T\{\sigma\} + \{\delta E\}^T\{D\}]\, dV = 0 \tag{11}$$

Using the of finite element formulation, the equation of motion for rectangular plate element subjected to a dynamic pressure and electrical field with aerodynamic damping are obtained as

$$\begin{bmatrix}[M] & 0\\ 0 & 0\end{bmatrix}\begin{Bmatrix}\ddot{W}\\ \ddot{W}_\emptyset\end{Bmatrix} + \begin{bmatrix}[G] & 0\\ 0 & 0\end{bmatrix}\begin{Bmatrix}\dot{W}\\ \dot{W}_\emptyset\end{Bmatrix} + \left(\lambda\begin{bmatrix}[A] & 0\\ 0 & 0\end{bmatrix} + \begin{bmatrix}[K] & [K_{w\emptyset}]\\ [K_{\emptyset w}] & [K_\emptyset]\end{bmatrix} + \begin{bmatrix}[K_1] & 0\\ 0 & 0\end{bmatrix} + \begin{bmatrix}[K_2] & 0\\ 0 & 0\end{bmatrix}\right)\begin{Bmatrix}W\\ W_\emptyset\end{Bmatrix} = \begin{Bmatrix}0\\ 0\end{Bmatrix} \tag{12}$$

Where,$[M]$,$[G]$, $[A]$, and $[K]$ are, mass, aerodynamic damping, aerodynamic influence, and linear stiffness matrices, respectively.$[K_1]$ and $[K_2]$ depend linearly and quadratically on element displacements respectively.$\{W_\emptyset\}$, $[K_{w\emptyset}]$, $[K_{\emptyset w}]$and $[K_\emptyset]$ are collected as the PZT elements work as actuators and sensors at the same time. Thus; the equations for self-sensing actuators are,

$$[M]\{\ddot{W}\} + [G(\lambda, C_a)]\{\dot{W}\} + (\lambda[A] + [K] + [K_1] + [K_2])\{W\} = -[K_{w\emptyset}]\{W_\emptyset\} \tag{13}$$

$$\begin{aligned}\{Q\} &= [K_{\emptyset w}]\{W\}\\ &= -[K_\emptyset]\{W_\emptyset\}\end{aligned} \tag{14}$$

Where; $\{\mathrm{Q}\}$ represents actuator and sensor collected vector charges $= \begin{Bmatrix}\mathrm{Q^a}\\ \mathrm{Q^s}\end{Bmatrix}$

$$\{W_\emptyset\} = \begin{Bmatrix}W_\emptyset^a\\ W_\emptyset^s\end{Bmatrix} \tag{15}$$

$$[K_\emptyset] = \begin{bmatrix}[K_\emptyset^a] & 0\\ 0 & [K_\emptyset^s]\end{bmatrix} \tag{16}$$

MODAL FORMULATION

To largely decrease the number of scalar equations to a fewer number, the modal

transformation is applied. This number equals to the participating modes number [24]

The bending displacements of the system as a linear combination of some known function are written as:

$$\{W\} = \sum_{r=1}^{n} q_r(t)\{\emptyset_r\} = [\emptyset]\{q\} \quad (17)$$

Where $\{\emptyset\}$ and$\{q\}$ are the element eigenvector and natural modal coordinate vector. The linear frequencies and the corresponding natural modes are obtained from the linear vibration of the system.

$$\omega_r^2[M]\{\emptyset_r\} = [K_b]\{\emptyset_r\} \quad (18)$$

Since the element nonlinear stiffness matrices can be expressed in terms of the element displacements $\{W_b\}$ and $\{W_m\}$, this displacement vector can be expressed by the linear modes$\{\emptyset_r\}$. The actuating equations of motion in modal coordinate become,

$$[\bar{M}]\{\ddot{q}\} + [\bar{G}]\{\dot{q}\} + \left([\bar{K}] + \left[\bar{K}_{qq}\right]\right)\{q\} = -\left[\bar{K}_{w\emptyset}^{a}\right]\{\bar{W}_{\emptyset}^{a}\} \quad (19)$$

For self-sensing actuators, $\left[\bar{K}_{w\emptyset}^{a}\right]$and $\{\bar{W}_{\emptyset}^{a}\}$are substituted by $[\bar{K}_{w\emptyset}]$ and $\{\bar{W}_{\emptyset}\}$. The sensing equation is

$$\{q^s\} = -\left[\bar{K}_{\emptyset w}^{s}\right]\{q\} \quad (20)$$

For self-sensing actuators, $\left[\bar{K}_{\emptyset w}^{s}\right]$ is substituted by $[\bar{K}_{\emptyset w}]$. In Eq. (19), the modal mass, linear stiffness and aerodynamic damping matrices are

$$([\bar{M}], [\bar{\mathrm{K}}], [\bar{\mathrm{G}}]) = [\emptyset]^{\mathrm{T}}(\bar{M}, [\mathrm{K}], [\mathrm{G}(\lambda, \mathrm{C_a})])[\emptyset]$$

The second order nonlinear modal stiffness matrix is

$$\left[\bar{K}_{qq}\right] = [\emptyset]^T \sum_{r=1}^{n}\sum_{s=1}^{n} q_r q_s \left([K_{2b}]^{rs} - [K1_{Nm}(\{W_m\}_2)]^{rs} - [K1_{bm}]^r [K_m]^{-1} [K1_{mb}]^s\right)[\emptyset] \quad (21)$$

The modal piezoelectric control force is

$$[\bar{K}_{w\emptyset}] = \begin{bmatrix}\left[\bar{K}_{w\emptyset}^{a}\right] \\ \left[\bar{K}_{w\emptyset}^{s}\right]\end{bmatrix} = [\emptyset]^T \begin{bmatrix}\left[K_{w\emptyset}^{a}\right] \\ \left[K_{w\emptyset}^{s}\right]\end{bmatrix} = [\emptyset]^T [K_{w\emptyset}] = [\bar{K}_{w\emptyset}]^T \quad (22)$$

CONTROL METHODOLOGY

Controller Design

A standard state space for control design and simulation can be written based on the modal Eq. (21), which represent the states are assigned the state vector X.

$$X=\begin{Bmatrix} q \\ \dot{q} \end{Bmatrix} \tag{23}$$

The state space form for the modal equations of motion is

$$\begin{aligned} \dot{X} &= \overline{A}(X,t)\, X + BU \\ Y &= CX + DU \end{aligned} \tag{24}$$

Where, U= $\{W_{\emptyset}\}$ is the control input.Y= $\{q^s\}$ is the sensor output.
The system matrices are

$$\begin{aligned} \overline{A} &= \begin{bmatrix} 0 & I \\ -[\bar{M}_b]^{-1}[\bar{K}] & -[\bar{M}_b]^{-1}[\bar{G}] \end{bmatrix} + \begin{bmatrix} 0 & I \\ -[\bar{M}_b]^{-1}\left[\bar{K}_{qq}(X,t)\right] & 0 \end{bmatrix} \\ B &= \begin{bmatrix} 0 \\ -[\bar{M}_b]^{-1}[\bar{K}_{b\emptyset}] \end{bmatrix},\ C = [-[\bar{K}_{b\emptyset}] \quad 0],\ D = 0 \end{aligned} \tag{25}$$

Where, $\overline{A}$ is a real system state matrix. $[\bar{K}_{b\emptyset}]$ exists for self-sensing actuators. We use its linearized form by applying Taylor series approach in designing a controller for the system. The second part of $\overline{A}$ represents the effect of nonlinear stiffness matrices of the panel. Using the linearization about the system reference point which, is the point with no deflection $\{q\}$ = 0. The second part of $\overline{A}$ can be neglected and the linearized result A matrix is the first part of $\overline{A}$ which is defined as:

$$A = \begin{bmatrix} 0 & I \\ -[\bar{M}_b]^{-1}[\bar{K}] & -[\bar{M}_b]^{-1}[\bar{G}] \end{bmatrix} \tag{26}$$

LQR Controller

A linear quadratic regulator (LQR) is used to design the full state feedback control for linear system and to get the gain values. The solution of the linear full state feedback using the (LQR) is written as:

$$U = -KX \tag{27}$$

Where, K represents the LQR gain vector.
U is used to minimize the quadratic performance index, A function J of both system states and control effort is given by,

$$J = \int_0^{\infty} [X^T Q X + U^T R U]\, dt \tag{28}$$

Where, *R* is a symmetric positive definite control effort-weighting matrix.
Q is a symmetric positive semi-definite state-weighting matrix.

The solution of the controller gains that minimizes the performance index is,

$$K = R^{-1}B^{T}P \quad (29)$$

Where, *P* is a positive definite symmetric matrix determined from the solution of the Riccati equation;

$$A^{T}\ P + PA - PBR^{-1}B^{T}P + Q = 0 \quad (30)$$

Modal Participation

The modal participation is used to determine the number of modes used (Abdel-Motagaly, Guo et al. 2005) which is expressed as:

$$P_{ar_{r-th}} = \frac{max|q_r|}{\sum_{s=1}^{n} max|q_s|} \quad (31)$$

Table 1 shows the modal participation values of the first four modes at various limit-cycle amplitudes for a simply supported square isotropic aluminum panel without piezoelectric material at different values of the non-dimensional aerodynamic pressure λ. Notice that our investigation is focused on λ = 1200 as will be discussed in details later.

Table 1 Modal Participation Values at Various Limit-Cycle Amplitudes

λ	w_{max}/Height	Modal Participation, %			
		q_{11}	q_{12}	q_{13}	q_{14}
600	0.35	30.9	30.9	18.7	9.35
800	0.645	40.9	40.3	13.2	3.0
1000	0.66	37.5	35.8	12.2	9.6

NUMERICAL SIMULATION OF PANEL FLUTTER AT VARIOUS FINITE ELEMENT MESHING SIZES

In this section, the effectiveness of LQR full state feedback on the panel flutter suppression at different FE meshing aspect ratios is investigated. The suitability of the aspect ratio is based on the higher control authority of the smaller PZT actuator size. The optimum actuator location to achieve the desired control authority is determined using the NFCG method.

The successful formation of the finite element model for a panel flutter problem depends on some factors that include; understanding of the physical problem including a qualitative knowledge of the structural response to be predicted, knowledge of the basic principles of mechanics and good understanding of the finite element procedures available for analysis.

Discretization of the domain into finite elements is the first step in the finite element formulation. The size, number and configuration of elements have to be chosen carefully such that the dynamic behavior of the studied panel is simulated as closely as possible without increasing the computational effort needed for the solution. The size of element influences the convergence of the solution directly and hence it has to be chosen carefully. The smaller the element size, the more accurate the solution we obtain and the larger the computational time to be consumed. Thus, a compromise should take place between meshing density and the accepted computational time especially the solution accuracy enhancement is not observed after certain finite element size. The meshing aspect ratio plays an essential rule in the accuracy of PZT optimum position for high control authority and the accurate PZT patch size sufficient to damp the flutter during the shortest time. Thus; the structural integrity is achieved and the fatigue effect is relieved. The aspect ratio is the ratio between the number of elements in both of the two perpendicular discretization directions (X-axis and Y-axis)

The studied panel is a standard simply supported square aluminum plate composing the fuselage of the highly maneuverable aircraft which. Piezoelectric patches is assumed to embedded with this panel. The properties of the hosting panel and the piezoelectric layer are listed in Table 2. The aircraft is assumed to move with a supersonic speed such that the panels are subjected to a non-dimensional aerodynamic pressure λ of 1200. According the dimensions and the properties of the hosting panel the critical non-dimensional aerodynamic pressure λ =512. The program was run at different aspect ratios. These aspect ratios are listed in Tables 3, 4, 5, 6 and 7. The total number of elements, the aspect ratios, and the element size are listed in each table. The total PZT areas along with the corresponding damping times are also listed in these tables for the sake of comparison.

Table 2. The material Properties of Isotropic Panel and PZT5A

Material	**Aluminum (Panel)**	**PZT5A (Actuator and Sensor)**
Thickness	h_s = 0.05 in	h_p = 0.015 in
Young's modulus	E_p = 10 Msi	E_e = 9 Msi
Mass density	$\rho_p = 0$ .2588×10^{-3} lb-sec^2/in^4	$\rho_e = 0.7101\times10^3$ lb-sec^2/in^4
Poisson's ratio	V_p=0.3	V_e =0.3
Charge Constant		d_{31}= -7.51×10^{-9} in/v, $d_{32} = d_{31}$, d_{36} = 0
Coercive Field		E_{max}=1.52×10^4 v/in

Table 3 Number of Elements in X is fixed at 8 and the Number of Elements in Y is Changed

No of Elements (X Direction)	**No of Elements (Y Direction)**	**Total Elements**	**N_X/N_Y**	**Size of one Element(in^2)**	**Damping Size(in^2)**	**Damping Time (s)**
8	4	32	2	4.5	9	0.076
8	8	64	1	2.25	4.5	0.039
8	10	80	0.8	1.8	7.2	0.085
8	12	96	2/3	1.5	9	0.078
8	14	112	0.571	1.285	10.28	0.065
8	16	128	0.5	1.125	11.25	0.063

Table 4. Number of Elements in X is fixed at 10 and the Number of Elements in Y is Changed

No of Elements (X Direction)	**No of Elements (Y Direction)**	**Total Elements**	**N_X/N_Y**	**Size of one Element(in^2)**	**PZT Size (in^2)**	**Damping Time (s)**
10	4	40	2.5	3.6	7.2	0.059
10	6	60	1.666	2.4	9.6	0.077
10	8	80	1.25	1.8	7.2	0.059
10	10	100	1	1.44	5.76	0.039
10	12	120	0.833	1.2	4.8	0.062
10	14	140	0.714	1.028	6.16	0.073
10	16	160	0.625	0.9	7.2	0.059
10	18	180	0.555	0.8	8	0.079
10	20	200	0.5	0.72	7.2	0.028

Table 5. Number of Elements in Y is fixed at 12 and the Number of Elements in X is Changed

No of Elements (X-Axis)	**No of Elements (Y-Axis)**	**Total Elements**	**N_X/N_Y**	**Size of one Element(in^2)**	***PZT* Size (in^2)**	**Damping Time (s)**
8	12	96	0.666	1.5	9	0.078
10	12	120	0.833	1.2	4.8	0.062
12	12	144	1	1	6	0.036
14	12	168	1.16	0.85	5.14	0.064
16	12	192	1.33	0.75	6	0.064
18	12	216	1.5	0.666	5.33	0.049

Table 6. Number of Elements in Y is fixed at 8 and the Number of Elements in X is Changed

No of Elements (X Direction)	**No of Elements (Y Direction)**	**Total Elements**	**N_X/N_Y**	**Size of one Element(in^2)**	***PZT* Size (in^2)**	**Damping Time (s)**
6	8	48	0.75	3	18	0.06
8	8	64	1	2.25	4.5	0.039
12	8	96	1.5	1.5	6	0.085
16	8	128	2	9/8=1.125	6.75	0.06
24	8	192	3	0.75	6	0.069

Table 7 Number of Elements in Y is Changed and the Number of Elements in X is Changed

No of Elements (X Direction)	**No of Elements (Y Direction)**	**Total Elements**	**N_X/N_Y**	**Size of one Element(in^2)**	***PZT* Size (in^2)**	**Damping Time (s)**
8	4	32	2	4.5	9	0.076
10	4	40	2.5	3.6	7.2	0.059
12	4	48	3	3	6	0.036
16	4	64	4	2.25	9	0.064
18	6	108	3	1.33	10.6	0.064
14	14	196	1	0.734	4.4	0.062

For the sake of absolute visual comparison and selection of the optimum aspect ratio, Figures 2, 3 and 4 are presented. In Figure 2, the size of PZT required for damping is plotted vs. the variation in Y-direction while keeping the number of elements in X-direction at fixed values. In case 1, the number of elements in X-direction is eight and in the second case, the number of elements in the same direction is 10. Figure 3 shows the relation between the PZT size and the variation in element number in X-direction, while the number of elements are kept fixed at certain value Y-direction. Figure 4 the size of PZT required for damping at different elements in X and Y direction.

The results shown in Table 3 and plotted in Figure 2 reveal that optimum aspect ratio is unity (8×8) where only two PZT elements of 4.5 in^2 total area are sufficient to damp the flutter after 0.039 s from its occurrence. The results shown in Table 4 reveal that the required PZT area for damping in case 10×12 is 4.8 in^2 and the corresponding damping time is 0.062 which is higher than that at 12×12 aspect ratio. it is noticed that the damping time is 0.036 at the latter meshing which is almost 50% of the damping time at 10×12 meshing. In Table 6, the case of 8×8 meshing is the same as that of Table 3. The results shown in table 6 reveal that the smallest PZT area sufficient to damp the vibration is at 14×14 meshing, where the damping time is 0.062 s. In the same table, the meshing 12×4 gives the shortest damping time with a larger PZT are at the latter case. As the damping times of the all investigated cases comparable and small, our main objective will be the area of the PZT actuator. From the above discussion, the recommended aspect ratio for accurate placement of high-control-authority PZT actuator is between 0.8 and 1.

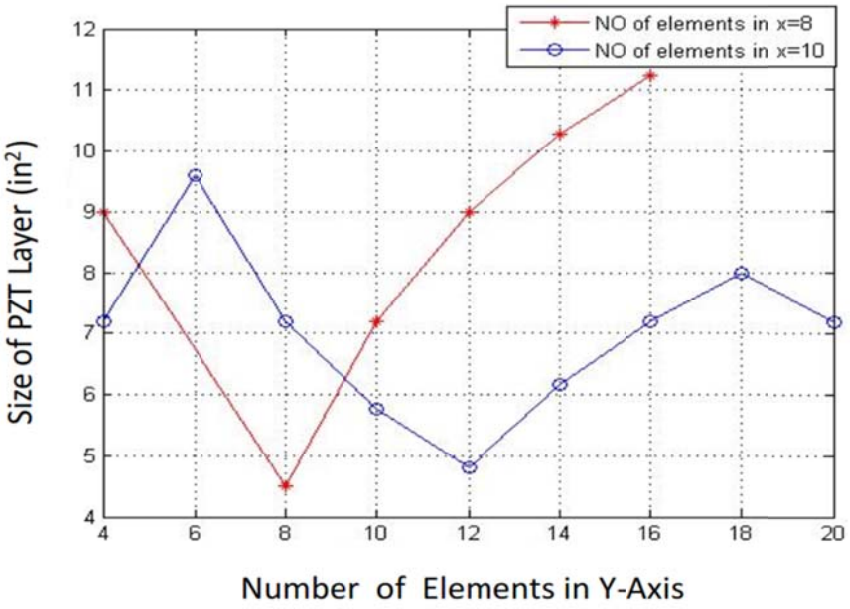

Figure 2. The size of PZT Actuator for Flutter Damping at Fixed Number of Elements in X Direction

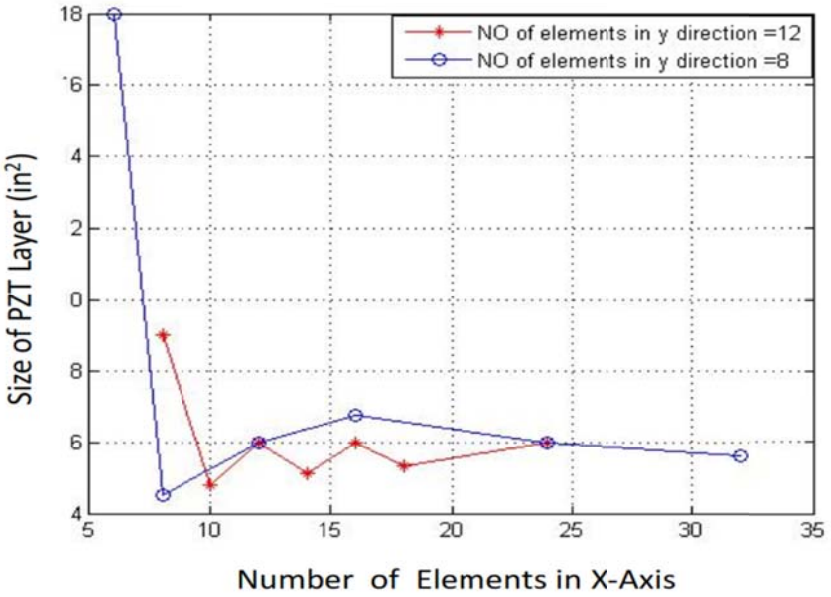

Figure 3 The size of PZT Actuator for Flutter Damping at Fixed Number of Elements in Y Direction

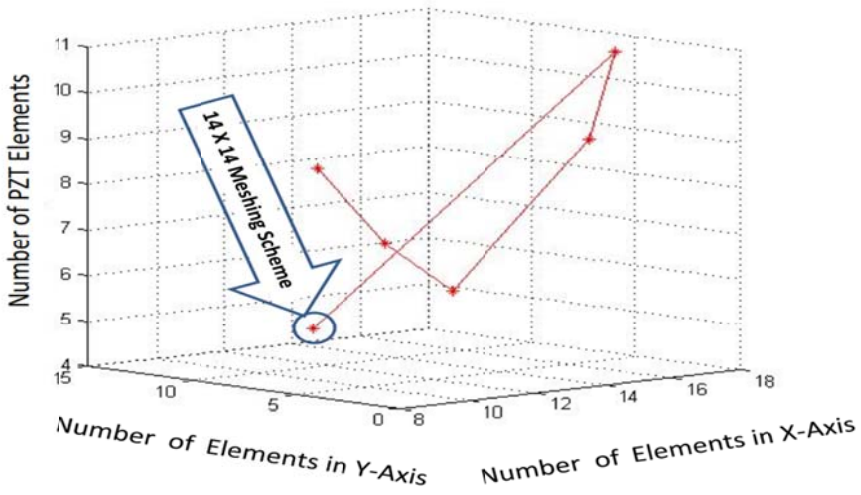

Figure 4 The size of PZT Actuator for Flutter Damping

The results of controlled lateral deflection at the various meshing discussed above are represented in Figures 4, 5 and 6. Figure 4 shows the controlled lateral deflection at 8×8 elements (aspect ratio of unity). Figure 5 shows the controlled lateral deflection at 10×12 elements (aspect ratio of 0.833). Figure 6 shows the controlled lateral deflection at 14×14 elements (aspect ratio of unity). In these figures, the actuator was turned on after 0.2 s of the fluttering occurrence and the complete damping is assumed to take place when the normalized lateral deflection of the panel becomes less than 0.05 where the damping time is recorded and listed in Tables 3-7.

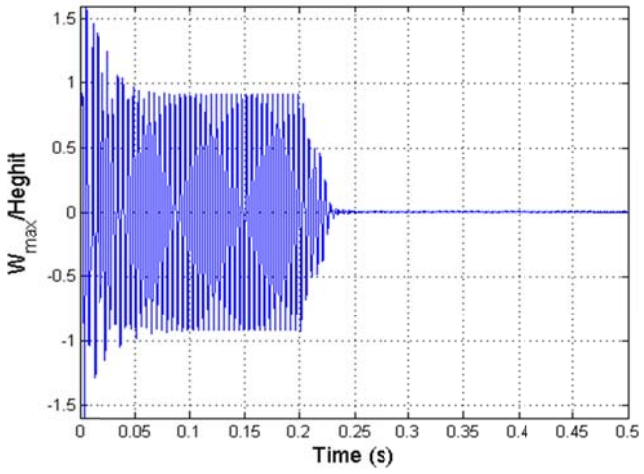

Figure 5 The Controlled Lateral Deflection of Fluttering Panel at 8×8 Meshing Size

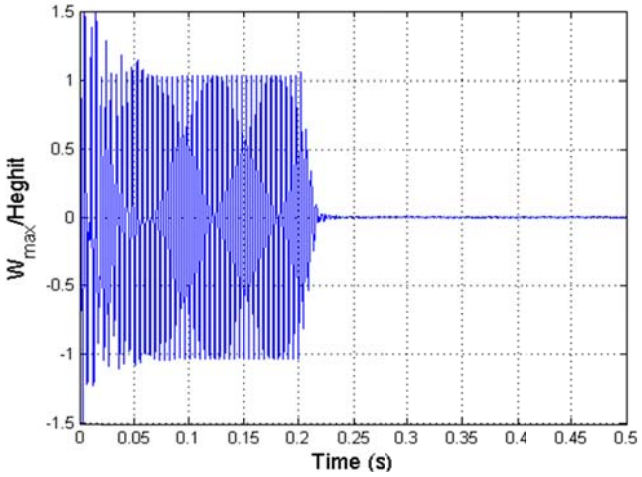

Figure 6. The Controlled Lateral Deflection of Fluttering Panel at 10×12 Meshing Size

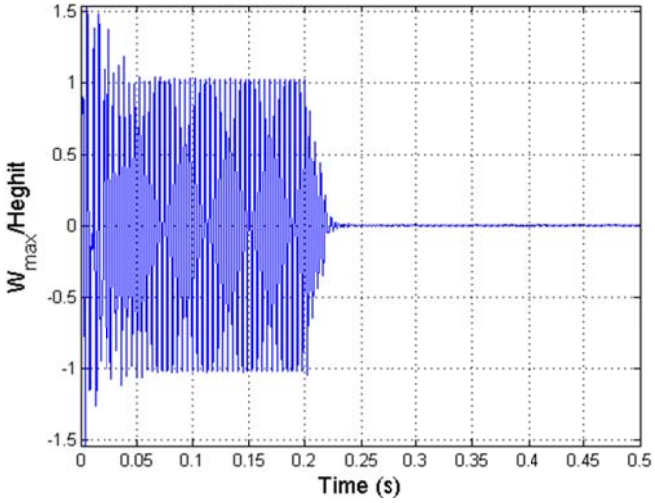

Figure 7 The Controlled Lateral Deflection of Fluttering Panel at 14×14 Meshing Size

PLACEMENT OF PIEZOELECTRIC ACTUATORS AT THE RECOMMENDED MESHING SIZES/ASPECT RATIOS

The optimal size and location of piezoelectric material for damping of panel flutter at the various FE meshing sizes, listed in Tables 3-7, are determined using the norms of feedback control gain (NFCG). The nondimensional aerodynamic pressure λ is assumed equal 1200. The recorded damping time and its corresponding PZT actuator size with smallest values of NFCG were extensively less than that of NFCG larger values. Thus, the NFCG norm values are calculated for each PZT assumed location and the locations with lower NFCG are selected to be the optimum candidate for placing the actuator locations

for actuators. The shadowed elements in Figures 8-10 represent the locations of PZT to achieve higher control authorities with smaller sizes of actuator as a result of using the recommended aspect ratio in finite element meshing formulation. It is common between figures that the control authority of the PZT actuator is augmented when the actuator is placed closer to the flow leading edge (LE) which is consistent with the reference [24]. Figure 8 shows the optimal PZT location in case of 8×8 meshing size. Figure 9 shows the optimal PZT location in case of 10×12 meshing size and Figure 10 shows the optimal PZT location in case of 14×14 meshing size.

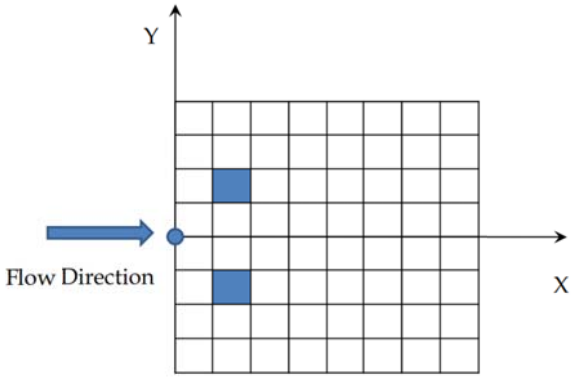

Figure 8 Optimal Location of PZT Actuator at 8×8 Meshing Size

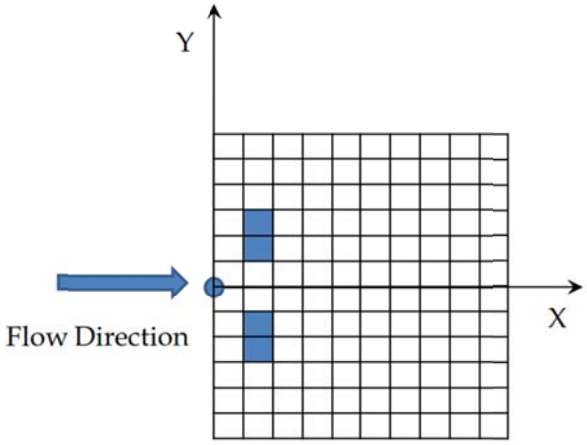

Figure 9 Optimal Location of PZT Actuator at 10×12 Meshing Size

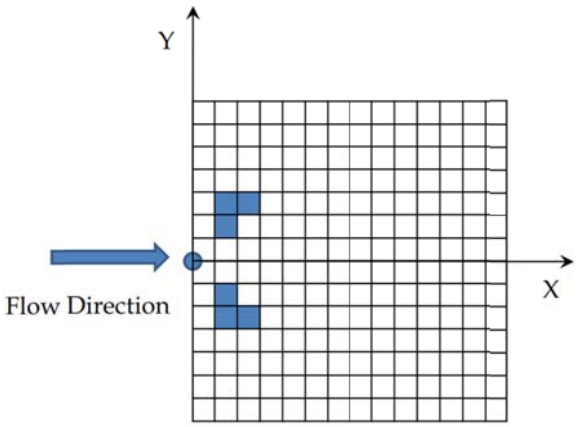

Figure 10 Optimal Location of PZT Actuator at 14×14 Meshing Size

CONCLUSIONS

The aspect ratio of the finite element meshing plays a vital rule in selecting the optimum position/area of the PZT actuator embedded with the hosting panel of highly maneuverable aircraft. it is recommend to use finer meshing size with aspect ratio between 0.8 and unity. Instead of using the bind iterative search method to select the optimum position of the PZT actuators, The LQR full state feedback could be used where the values of the NFCG will guide us to the elected spots for PZT actuators with higher control authorities.

REFERENCES

Abdel-Motagaly, K. (2001). "FINITE ELEMENT ANALYSIS AND ACTIVE CONTROL FOR NONLINEAR FLUTTER OF GOMPITE PANELS UNDER YAWED SUPERSONIC FLOW." DOCTOR of philosophy (Aerospace Engineering Old Dominion University).

Abdel-Motagaly, K., X. Guo, et al. (2005). "Active Control of Nonlinear Panel Flutter Under Yawed Supersonic Flow." AIAA Journal **43**(3): 671-680.

Bin Zheng , J. Y. (2012). "vibration analysis of base structure on SINS using PZT actuators." Eng & Comp Science **20**.

Chowdary, T. V. R., S. Parthan, et al. (1994). "Finite element flutter analysis of laminated composite panels." Computers & Structures **53**(2): 245-251.

Forster, E. E. and H. T. Y. Yang (1998). "Flutter Control of Wing Boxes Using Piezoelectric Actuators." Journal of Aircraft **35**(6): 949-957.

Johns, D. J. (1965). "A SURVEY ON PANEL FLUTTER." Presented at the 21st Meeting of the AGARD Structures and Materials Panel
in Nancy,(NORTH ATLANTIC TREATY ORGANIZATION
ADVISORY GROUP FOR AEROSPACE RESEARCH AND DEVELOPMENT).

Lee, Y. Y., K. K. Yuen, et al. (2002). "Numerical simulation model of vibration responses of rectangular plates embedded with piezoelectric actuators." Thin-Walled Structures **40**(1): 1-28.

Li, F.-M. (2012). "Active aeroelastic flutter suppression of a supersonic plate with piezoelectric material." International Journal of Engineering Science **51**(0): 190-203.

Li, F.-M. and Z.-G. Song (2013). "Flutter and thermal buckling control for composite laminated panels in supersonic flow." Journal of Sound and Vibration **332**(22): 5678-5695.

Li, J. and Y. Narita (2013). "Analysis and optimal design for supersonic composite laminated plate." Composite Structures **101**(0): 35-46.

lock, m. h. (1961). "a study of two-dimensional panel flutter." california institute of techenology(doctor of philosophy).

M. Lotfy, M. E. (2009). "Active Composite Panel Flutter using Finite Element Method." AEROSPACE SCIENCES & AVIATION TECHNOLOGY, **ASAT-13-ST-25**.

Mei, C., K. Abdel-Motagaly, et al. (1999). "Review of Nonlinear Panel Flutter at Supersonic and Hypersonic Speeds." Applied Mechanics Reviews **52**(10): 321-332.

Moon, S., C. Yun, et al. (2002). "Passive suppression of nonlinear panel flutter using piezoelectric materials with resonant circuit." KSME International Journal **16**(1): 1-12.

Moon, S. H. (2006). "Finite element analysis and design of control system with feedback output using piezoelectric sensor/actuator for panel flutter suppression." Finite Elements in Analysis and Design **42**(12): 1071-1078.

Otiefy, R. A. H. and H. M. Negm (2011). "Wing box transonic-flutter suppression using piezoelectric self-sensing diagonal-link actuators." International Journal of Solids and Structures **48**(1): 31-43.

Pidaparti, R. M. V. (1993). "Flutter analysis of cantilevered curved composite panels." Composite Structures **25**(1–4): 89-93.

qinqin (2005). "active control of large amplitude nolinear free vibrations and nonlinear supersonic panel flutter of beams and composite plates using piezoelectric self-sensing actuator." old dominion university master science thesis.

Raja, S., A. A. Pashilkar, et al. (2006). "Flutter control of a composite plate with piezoelectric multilayered actuators." Aerospace Science and Technology **10**(5): 435-441.

S.X. Xu, T. S. K. (2004). "Finite element analysis and design of actively controlled piezoelectric smart structures " Finite Elements in Analysis and Design **40**(Research and Emerging Technologies Department, Canada): 241–262.

Sallam ahmed kouritem, M. M. Y. B. E., Hassan Anwar El-Gamal (2013). "An Ad-Hock Methodology for Optimal Placement/Area of PZT for Flutter Damping." International Journal of Scientific & Engineering Researc **4**(12).

Vedeneev, V. V. "Effect of damping on flutter of simply supported and clamped panels at low supersonic speeds." Journal of Fluids and Structures(0).

Yucheng Shi, R. Y. Y. L. C. M. (1999). "THERMAL POSTBUCKLING OF COMPOSITE PLATES USING THE FINITE ELEMENT MODAL COORDINATE METHOD." Journal of Thermal Stresses **22**(6): 595-614.

Zhou, R. C., C. Mei, et al. (1996). "Suppression of nonlinear panel flutter at supersonic speeds and elevated temperatures." AIAA Journal **34**(2): 347-354.

Zhou, R. C., D. Y. Xue, et al. (1994). "Finite element time domain - Modal formulation for nonlinear flutter of composite panels." AIAA Journal **32**(10): 2044-2052.